Desalination and Water Treatment
www.deswater.com

doi:10.5004/dwt.2016.0048

59 (2017) 99–113
January

Johannesburg-sulfur autotrophic denitrification system treatment of municipal wastewater with a low COD/TN ratio: Performance, material balance and bacterial community

Haibo Li[a,b,c], Beihai Zhou[a,*], Zhiyong Tian[b,c,*], Yonghui Song[b,c], Huibin Yu[b,c], Liancheng Xiang[b,c], Siyu Wang[b,c], Chen Sun[b,c]

[a]*Department of Environmental Engineering, School of Civil and Environmental Engineering, University of Science and Technology Beijing, Xueyuan road 30#, Beijing, 100083, China, Tel. +86 15652933695; email: lhb19850725@163.com (H. Li), Tel. +86 10 62334821; email: zhou_beihai@126.com (B. Zhou)*

[b]*State Key Laboratory of Environmental Criteria and Risk Assessment, Chinese Research Academy of Environmental Sciences, Dayangfang 8#, Anwai Beiyuan, Beijing 100012, China, Tel. +86 18612834618; email: hkytzy2008@163.com (Z. Tian), Tel. +86 10 84924787; email: songyh@craes.org.cn (Y. Song), Tel. +86 15810987118; email: yhbybx@163.com (H. Yu), Tel. 13701249720; email: xianglc@craes.org.cn (L. Xiang), Tel. +86 13501010037; email: wangsiyu268@163.com (S. Wang), Tel. +86 18624321558; email: sunchen@craes.org.cn (C. Sun),*

[c]*Department of Urban Water Environmental Research, Chinese Research Academy of Environmental Sciences, Dayangfang 8#, Anwai Beiyuan, Beijing 100012, China*

Received 12 January 2016; Accepted 2 July 2016

ABSTRACT

The simultaneous nitrogen and phosphorus removal performance of the Johannesburg-Sulfur autotrophic denitrification (JHB-SAD) system was investigated in this study. The results showed that the JHB-SAD system achieved maximum removal efficiencies of 86.5, 96.0, 96.4 and 90.7% for COD, TN, NH_4^+–N and TP, respectively, with average effluent concentrations of 27.7, 1.26, 0.99 and 0.18 mg L^{-1}, respectively. These results indicate that the nutrients could be almost completely removed by the JHB-SAD system if NH_4^+–N was sufficiently oxidized and that the JHB-SAD system could be a promising alternative to remove nutrients from municipal wastewater with a low COD/TN ratio. Meanwhile, bacterial communities in the JHB-SAD system were investigated using high-throughput sequencing technology. Taxonomic analysis found that 8 abundant phyla in the JHB-SAD system accounted for 86.8–91.1% of the total effective sequences, which were *Proteobacteria* (34.7–57.5%), *Bacteroidetes* (11.7–23.4%), *Planctomycetes* (8.71–20.1%), *Chloroflexi* (3.08–9.42%), *Firmicutes* (1.83–3.00%), *Verrucomicrobia* (0.41–1.81%), *Gemmatimonadetes* (0.44–1.27%) and *Chlorobi* (0.30–1.05%). In addition, redundancy analysis (RDA) showed that the phyla *Bacteroidetes*, *Chlorobi*, and *Firmicutes* were related to COD, NH_4^+–N concentration and COD removal, and the phyla *Gemmatimonadetes* and *Chloroflexi* were related to the SO_4^{2-} concentration in the SAD reactor due to autotrophic denitrification.

Keywords: Wastewater with a low COD/TN ratio; Efficient nutrients removal; Johannesburg-Sulfur autotrophic denitrification system (JHB-SAD); High-throughput sequencing; Redundancy Analysis (RDA)

*Corresponding authors.

1. Introduction

With the development of industry and agriculture, the excessive discharge of nutrients (particularly nitrogen and phosphorus) has attracted increasing attention globally [1–3]. Nutrients can cause eutrophication of the water environment and deterioration of water quality, thus posing a threat to human health [4–6]. Therefore, more stringent effluent quality standards are being implemented that require more effective nutrients removal for municipal wastewater treatment plants (WWTPs). However, the ratio of chemical oxygen demand to total nitrogen (COD/TN) in WWTP influent is usually low (4–6), which is a disadvantage for effective nutrients removal. Nutrients removal in conventional WWTPs involves several complex biochemical reactions, such as biodegradation, nitrification, denitrification, anaerobic phosphorus release and aerobic phosphorus uptake [7,8]. There are three main contradictions in simultaneous nitrogen and phosphorus removal via an anaerobic-anoxic-aerobic system: the shortage of organic carbon in the influent; NO_3^-–N in the return sludge; and the conflicting sludge retention time (SRT) between nitrifiers and polyphosphate-accumulating organisms (PAOs) [9–11]. Although widely applied in existing WWTPs, several biological nutrients removal (BNR) processes are unreliable in the simultaneous removal of nitrogen and phosphorus pollutants due to the shortage of organic carbon.

Advanced wastewater treatment technologies and processes, such as the signal reactor for high-activity ammonia removal over nitrite (SHARON) [12,13], shortcut nitrification–denitrification [14,15] and anammox [16,17], have been developed to solve the problem of nitrogen removal from wastewater with a low COD/TN ratio. However, these processes require precise operational conditions, including pH, alkalinity, temperature and dissolved oxygen [16–18]. In addition, phosphorus removal has been neglected in advanced wastewater treatment. Furthermore, the efficiency of nitrogen removal via conventional nitrification–denitrification or shortcut nitrification–denitrification cannot reach 100% even with sufficient amounts of influent organic carbon, because the nitrogen removal efficiency depends on the nitrate recycling ratio (r) and the sludge return ratio (R), which is $(R+r)/(1+R+r)$. Although the five-stage Bardenpho process is theoretically capable of achieving complete nitrogen removal, it is difficult to realize in practice without an influent TKN/COD ratio greater than 0.09 mgN/mgCOD [11]. In contrast, the anammox process can remove a maximum of only 88.7% nitrogen based on chemometrics [11].

Recently, Li et al. [19] developed an efficient nitrogen removal system that integrated the Johannesburg process (JHB) and the sulfur autotrophic denitrification process (SAD) to treat municipal wastewater with a low COD/TN ratio. In this novel system, the JHB process was primarily employed for organic carbon biodegradation, nitrification and heterotrophic denitrification. Meanwhile, the SAD process was employed for autotrophic denitrification to further remove the nitrate that is not removed in the JHB process due to a shortage of organic carbon. The average nitrogen removal efficiency of the JHB-SAD system could reach 94% under a COD/TN ratio of 4–5. However, no study on the phosphorus removal performance of the JHB-SAD system has been performed. Moreover, H^+ was produced during the SAD process. In addition, the composition of the bacterial community in the JHB-SAD system was required for a thorough investigation to better understand the characterization of the bacterial ecosystem.

In this study, the simultaneous removal of nitrogen and phosphorus pollutants in the JHB-SAD system was analyzed via calculation of the material balance. Moreover, limestone and dolomite were filled into SAD reactors to adjust the pH value of SAD effluent. In addition, high-throughput sequencing, which is considered a powerful method to investigate the microbial community in sludge samples of various wastewater treatment processes [20,21], was performed in different zones of the JHB-SAD system to evaluate the bacterial communities. The relationship between the phylum abundance and the environmental parameters was also evaluated by redundancy analysis. The objective of this study is to provide a firm understanding of the novel JHB-SAD system for the treatment of municipal wastewater with a low COD/TN ratio.

2. Experimental methods and materials

2.1. Experimental system set-up

According to the discharge standard of pollutants for a municipal wastewater treatment plant in China (GB-18918-2002), Shenyang north wastewater treatment plant must be upgraded. Based on the original SDAO system, the JHB-SAD system was set up in the Shenyang north wastewater treatment plant in Shenyang City, Liaoning Province, China, to effectively remove organic matter, nitrogen and phosphorus from municipal wastewater with a low COD/TN ratio. The layout and schematic diagram of the JHB-SAD system are shown in Fig. 1. The JHB system consisted of a pre-anoxic zone (PAN, volume of 0.83 $m^{3)}$, an anaerobic zone (ANA, volume of 1.61 m^3), an anoxic zone (ANO, volume of 1.16 m^3), an aerobic zone (AE, volume of 2.77 m^3), and a secondary settler (SES, working volumes of 1.07 m^3). The ANA and PAN in the JHB process were derived from the primary settler and the sludge recovery zone in the original wastewater treatment system. Due to a shortage of organic carbon for heterotrophic denitrification, the SAD process was proposed to improve nitrogen removal performance. The effluent of the JHB process was pumped into four up-flow SAD reactors. The height and inner diameter of all SAD reactors were 75 cm and 14 cm, respectively. The packing height of all SAD reactors was 70 cm. SAD reactor S1# was filled with granular sulfur (equivalent diameter of 3–4 mm), with a porosity of 47.3%. Due to the H^+ produced by the SAD process, limestone and dolomite were filled into SAD reactors S2#–S4# with granular sulfur. The neutralizing H^+ effect of limestone was investigated via SAD reactors S2#–S3#. Granular sulfur (3–4 mm) and limestone (0.8–1.2 mm) were filled into SAD reactors S2# (mass ratio 2:1) and S3# (mass ratio 1:1) with the porosity of 45.7 and 43.5%, respectively. However, Ca^{2+} was produced in the neutralization because the main

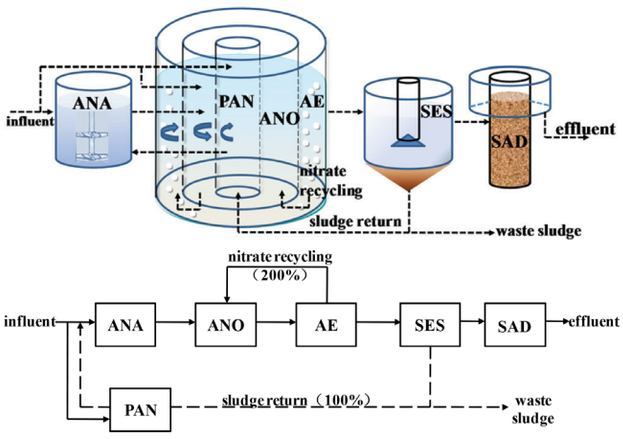

Fig. 1. Layout (a) and schematic diagram (b) of the JHB-SAD system. PAN: pre-anoxic zone; ANA: anaerobic zone; ANO: anoxic zone; AE: aerobic zone; SES: secondary settler; SAD: sulfur autotrophic denitrification reactor.

composition of limestone is calcium carbonate. Simultaneously, sulfate was produced in the SAD process. A calcium sulfate covering was formed on the granular sulfur surface if the sulfate concentration was high. Therefore, dolomite was used as an alternative because it is mainly composed of calcium carbonate and magnesium carbonate ($CaCO_3 \cdot MgCO_3$). The neutralizing effect of dolomite was investigated via SAD S4# reactor. SAD reactor S4# was filled with granular sulfur (3–4 mm) and dolomite (0.8–1.2 mm), and the mass ratio of sulfur to dolomite was 2:1 with a porosity of 45.7%.

2.2. Wastewater source and seed sludge

The experiment was conducted at the Guodian Shenyang northern wastewater treatment plant in Shenyang City, Liaoning Province, China. The raw wastewater from the WWTP sewer line was pumped into the pilot-scale JHB-SAD system. The characteristics of raw wastewater were as follows: chemical oxygen demand (COD) of 145.3 ± 39.2 mg L^{-1}, total nitrogen (TN) content of 30.9 ± 4.0 mg L^{-1}, ammonia (NO_4^-–N) content of 25.4 ± 4.8 mg L^{-1}, and phosphate (TP) content of 1.72 ± 0.77 mg L^{-1}. The influent COD/TN ratio was approximately 4–5, which is typical of municipal wastewater with a low COD/TN ratio. The seed sludge of JHB and SAD reactor S1# were collected from the full-scale wastewater treatment system where the nutrients removal was inefficient. The seed sludge of SAD reactors S2#-S4# were collected from S1#.

2.3. Analytical methods

Nitrate (NO_3^-–N), nitrite (NO_2^-–N), NH_4^+–N, TN, TP, sulfate (SO_4^{2-}) and mixed liquor suspended solid (MLSS) were analyzed according to standard methods [22]. COD was measured using a Lian-hua COD quick-analysis apparatus (Lian-hua Tech Co., Ltd, China). Dissolved oxygen (DO) and temperature were determined using a WTW Oxi 3310 meter with DO and temperature probes (WTW Company, Germany). The pH value was monitored by a WTW Multi 3420 meter with a pH electrode (WTW Company, Germany).

2.4. Experimental procedure

From December 18, 2013 to May 12, 2014, the pilot system was operated for 137 d, including four experimental phases. In phase I (days 1–31) and phase II (days 32–76), the performance of the JHB-SAD system and step-feed JHB-SAD system was evaluated for efficient nitrogen removal from municipal wastewater with a low COD/TN ratio. In phase III (days 77–104) and phase IV (days 105–132), sodium acetate (COD of 40 mg L^{-1}) was added to improve the nutrients removal performance of the JHB-SAD system and the step-feed JHB-SAD system.

The inflow was maintained at 0.56 m^3 h^{-1} during the different experimental periods. The MLSS were controlled at 2500–2700 mg L^{-1}. Using discharging waste sludge, the SRT was controlled on days 17–23 with sodium acetate dosing and on days 27–33 for normal operation. The nitrate recycling ratio (r) and sludge return ratio (R) were set to 200 and 100%, respectively, during the experimental phases. DO was controlled at 2.0–2.5 mg L^{-1} in the aerobic zone. The influent distribution ratio of the pre-anoxic zone and anaerobic zone was 30 and 70%, respectively, for the JHB-SAD system (phase I and phase III). For the step-feed JHB-SAD system (phase II and phase IV), the influent distribution ratios of the pre-anoxic zone, anaerobic zone and anoxic zone were 30, 40 and 30%, respectively.

The acclimation process of SAD reactors is briefly described in here. First, the tap water was used to make up the SAD influent. Then, half tap water and half second settler effluent were mixed and used to make up the SAD influent. The influent nitrate concentration was maintained at 15 mg L^{-1}, and the actual hydraulic retention time (AHRT) was set to 25 min during sludge acclimation. When the nitrate content was decreased to 2–3 mg L^{-1}, the next acclimation step was performed. In the experimental phase, JHB and SAD processes were integrated to treat municipal wastewater with a low COD/TN ratio. The AHRT of SAD reactor S1# was set to 25 min (days 1–7). Then, it was decreased to 15 min for days 8–19 and 10 min for days 20–31. During phase II–phase IV, SAD reactors S2#–S4# were run to regulate the pH of the JHB-SAD system effluent. The AHRT of all four SAD reactors was 10 min. the AHRT was calculated according to formula (1).

$$\mathrm{AHRT} = \frac{\mathrm{V} \times \eta}{\mathrm{Q}} \quad (1)$$

where V is the empty bed working volume of SAD reactors; Q represents the influent flows of the SAD reactor; and η denotes the porosity of the SAD reactors. AHRT shows the actual reaction time of the SAD process.

2.5. The calculations of pollutant removal capacity in different zones of the JHB-SAD system

Based on the material balance, the COD, nitrogen and TP removal capacity along the JHB-SAD system were calculated according to Eqs. (2)–(7):

Pre-anoxic zone:

$$Q_{PAN}\cdot C_{\inf.C,N,P}+Q_R\cdot C_{SES.C,N,P}= \left(Q_{PAN}+Q_R\right)\cdot C_{PAN.C,N,P}+\Delta S_{PAN.C,N,P} \quad (2)$$

Anaerobic zone:

$$Q_{ANA}\cdot C_{\inf.CNP}+\left(Q_{PAN}+Q_R\right)\cdot C_{PAN.C,N,P=} \left(Q_{PAN}+Q_{ANA}+Q_R\right)\cdot C_{ANA.C,N,P}+\Delta S_{ANA.C,N,P} \quad (3)$$

Anoxic zone:

$$Q_{ANO}\cdot C_{\inf.C,N,P}+\left(Q_{PAN}+Q_{ANA}+Q_R\right) \cdot C_{ANA.C,N,P}+Q_r\cdot C_{AE.C,N,P}= \left(Q_{PAN}+Q_{ANA}+Q_{ANO}+Q_R+Q_r\right)\cdot C_{ANO.C,N,P}+\Delta S_{ANO.C,N,P} \quad (4)$$

Aerobic zone:

$$Q_{ANO}\cdot C_{\inf.C,N,P}+\left(Q_{PAN}+Q_{ANA}+Q_R\right) \cdot C_{ANA.C,N,P}+Q_r\cdot C_{AE.C,N,P}= \left(Q_{PAN}+Q_{ANA}+Q_{ANO}+Q_R+Q_r\right) \cdot C_{ANO.C,N,P}+\Delta S_{ANO.C,N,P} \quad (5)$$

Secondary settler

$$\left(Q_{PAN}+Q_{ANA}+Q_{ANO}+Q_R\right)\cdot C_{AE.C,N,P}= \left(Q_{PAN}+Q_{ANA}+Q_{ANO}+Q_R\right)\cdot C_{SES.C,N,P}+\Delta S_{SES.C,N,P} \quad (6)$$

SAD reactor:

$$\left(Q_{PAN}+Q_{ANA}+Q_{ANO}\right)\cdot C_{SES.C,N,P}= \left(Q_{PAN}+Q_{ANA}+Q_{ANO}\right)\cdot C_{SAD.C,N,P}+\Delta S_{SAD.C,N,P} \quad (7)$$

where Q_{PAN}, Q_{ANA} and Q_{ANO} are the influent flows of the pre-anoxic, anaerobic and anoxic zones, respectively; Q_R and Q_r represent the sludge return flow and nitrate recycling flow, respectively; $C_{inf.C,N,P}$, $C_{PAN.C,N,P}$, $C_{ANA.C,N,P}$, $C_{ANO.C,N,P}$, $C_{AE.C,N,P}$, $C_{SES.C,N,P}$, and $C_{SAD.C,N,P}$, denote pollutant concentrations in the influent, pre-anoxic zone, anaerobic zone, anoxic zone, aerobic zone, secondary settler and SAD reactor, respectively; and $\Delta S_{PAN.C,N,P}$, $\Delta S_{ANA.C,N,P}$, $\Delta S_{ANO.C,N,P}$, $\Delta S_{AE.C,N,P}$, $\Delta S_{SES.C,N,P}$, and $\Delta S_{SAD.C,N,P}$, are the capacity of pollutants changed in the pre-anoxic zone, anaerobic zone, anoxic zone, aerobic zone, secondary settler and SAD reactor, respectively. Eqns. (2)–(7) were used in Fig. 5 to calculate the amount of COD and nitrogen and TP removal in the different units of the JHB-SAD system.

2.6. Bacterial community analysis

2.6.1. DNA extraction, PCR amplification and sequencing

To investigate the bacterial community in the JHB-SAD system, sludge samples of the pre-anoxic zone, anaerobic zone, anoxic zone, aerobic zone and SAD reactor S3# were obtained on day 132. The genomic DNA was extracted from 0.2 g sludge samples using an E.Z.N.A. Soil DNA Kit D5625-01 (Omega, USA) according to the manufacturer's protocol. To confirm the dosing quantity of DNA in the PCR reaction, DNA was accurate quantified using a Qubit 2.0 DNA Assay Kit Q10212 (Life, USA).

The V3–V4 region 16S rRNA genes were amplified from the genomic DNA via primer pairs 341F/805R for bacteria containing the Miseq sequencing platform universal adaptors. The fusion primer pairs 341F and 805R were 5′-ccctacacgacgctcttccgatctgCCTACGGGNGGCWGCAG-3′ and 5′-gactggagttccttggcacccgagaattccaGACTACHVGGGTATCTAATCC-3′, where the adaptors are shown in lowercase letters. The nucleotide barcodes that allow sample multiplexing during the sequencing were inserted between the adaptors and the primers. The first-round PCR reactions were performed in 50 µl of PCR mixture containing 5 µl of 10 × PCR buffer, 0.5 µl of 10 nM dNTPs, 10 ng of genomic DNA, 0.5 µl of each primer (50 µM), 0.5 µl of 5U/µl Platinum Taq DNA Polymerase Ep0406 (Thermo, USA) and ddH_{2O} added to 50 µl. The conditions of the first-round PCR were listed as follows: 94°C for 3 min, followed by 5 cycles at 94°C for 30 s, 45°C for 20 s, 65°C for 30 s, then 20 cycles at 94°C for 20 s, 55°C for 20 s, 72°C for 30 s and a final extension at 72°C for 5 min. The second-round PCR reactions were then performed in 50 µl of PCR mixture containing 5 µl of 10 × PCR buffer, 0.5 µl of 10 nM dNTPs, 20 ng of DNA, 0.5 µl of each primer (50 µM), 0.5 µl of 5U/µl Platinum Taq DNA Polymerase Ep0406 (Thermo, USA) and ddH2O add to 50 µl. The conditions of the second-round PCR were as follows: 95°C for 30 s, followed by 5 cycles at 95°C for 15 s, 55°C for 15 s, 72°C for 30 s and a final extension at 72°C for 5 min.

The PCR products were pooled and purified by a SanPrep DNA Gel Extraction Kit SK8192 (Sangon Biotech, China), and the concentrations of purified products were quantified by a Qubit2.0 DNA Assay Kit Q10212 (Life, USA) and then were mixed in equal amounts based on DNA concentration, followed by sequencing on the Miseq sequencing platforms (Illumina, USA) by Sangon Biotech (Sangon Biotech (Shanghai) Co., Ltd., China). After sequencing, the low-quality sequences, adapter primers, barcodes and primers were removed from the resulting sequences. The treated sequences were then checked, and the chimeric sequences were filtered out by a Chimera Slayer in the Mothur package. The remaining sets of sequences were formed into effective sequences. Sequencing produced 23,941 (pre-anoxic zone), 16,387 (anaerobic zone), 25,398 (anoxic zone), 22,077 (aerobic zone) and 20,832 (SAD reactor S3#) high-quality V3–V4 regions of the 16S rRNA gene for bacteria.

2.6.2 Biodiversity analysis and phylogenetic taxonomy

The effective sequences were clustered into operational taxonomic units (OTUs) by setting a 97% similarity using the Ribosomal database project (RDP) classifier. Based on the OTUs, the coverage percentage, abundance-based coverage

estimator (ACE), Chao1 richness estimator and Shannon diversity indices were calculated in the Mothur software program for each sample. To identify the species, the representative sequences from each OTU were compared to the entries in the SILVA database with a confidence threshold of 80%. In addition, redundancy analysis (RDA) [23] was used to evaluate the relationship between the phylum abundance and the environmental parameters via the R software program.

3. Results and discussion

3.1. Performance of the processes

3.1.1. Pollutant removal in the JHB-SAD system

The COD and nutrients removal performance of the JHB-SAD system in phases I–II are shown in Fig. 2. Fig. 2(a) and Fig. 2(b) indicate that the performance of COD and NH_4^+–N removal was excellent in phases I–II. The average influent COD and NH4$^+$–N concentrations were 138 mg L^{-1} and 24 mg L^{-1}, respectively. The average JHB-SAD system effluent concentrations of COD and NH4$^+$–N were 21.9 mg L^{-1} and 1.0 mg L^{-1}, respectively, with corresponding removal efficiencies of 84.1 and 95.8%. The COD was effectively removed and was maintained at a low level. Moreover, the NH4$^+$–N concentration observably decreased to 1–2 mg L^{-1} in the aerobic zone (Fig. 3(a, b)). In addition, approximately 9 mg L^{-1} COD and 0.6 mg L^{-1} NH4$^+$–N were removed by the filtration of sulfur granules and the assimilation of sulfur autotrophic bacteria under the SAD process (Fig. 2(a, b)).

Fig. 2(c) and Fig. 3 show that the JHB process effluent TN and NO_3^-–N concentrations were 13.8 mg L^{-1}, 11.6 mg L^{-1} (phase I) and 14.3 mg L^{-1}, 11.9 mg L^{-1} (phase II), respectively. In the units of the JHB process, the TN concentration was maintained at 11 to 14 mg L^{-1} (Fig. 2(c)).

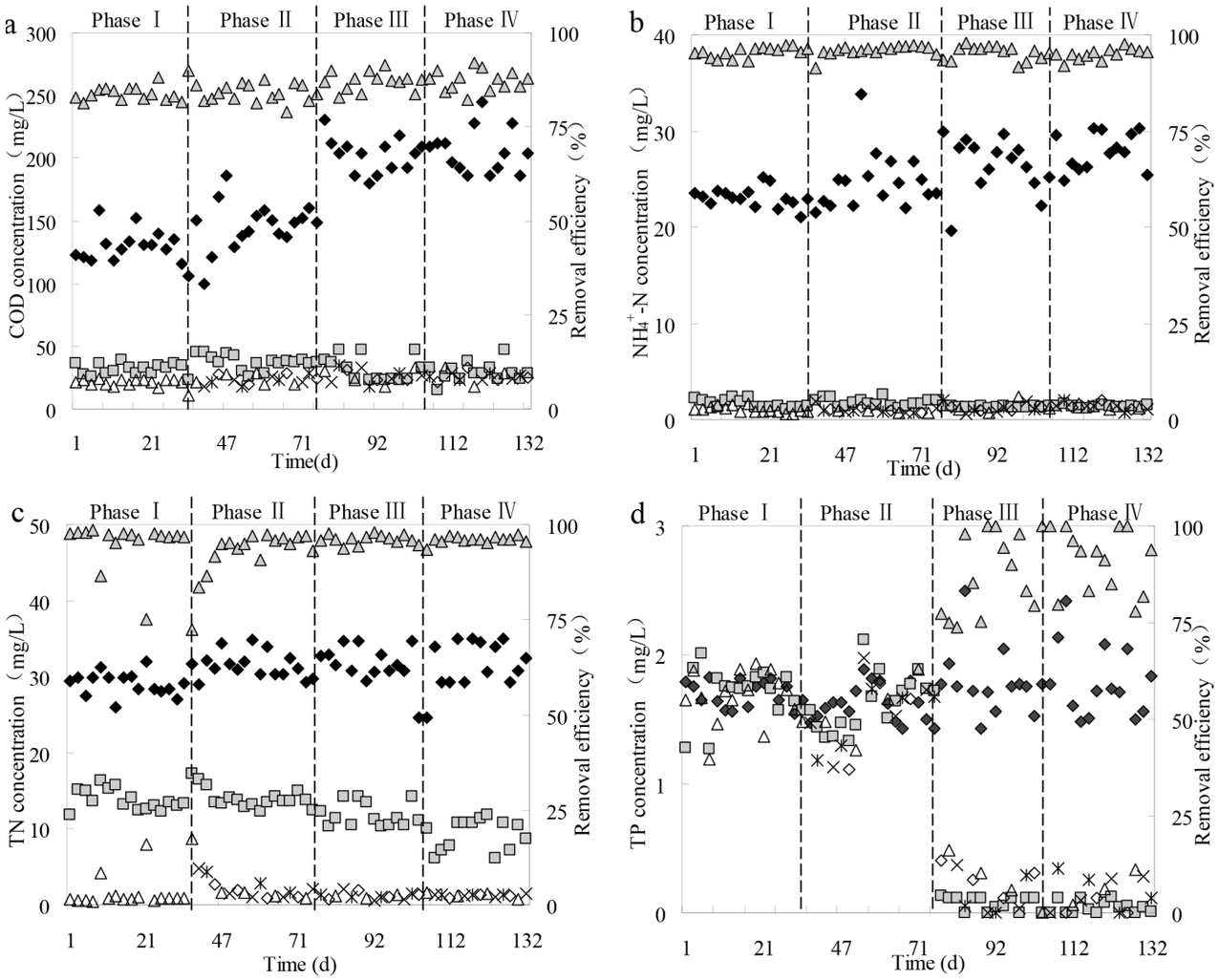

◆: influent; ■: effluent from secondary sedimentation tank; ▲: removal efficiency; △: SAD S1# effluent; ×:SAD S2# effluent; ✳: SAD S2# effluent; ◇: SAD S4# effluent

Fig. 2. Performance of (a) COD removal, (b) NH4$^+$-N removal, (c) TN removal and (d) TP removal in the JHB-SAD system during phase I–phase IV.

However, the TN compositions were different in each zone, as shown in Fig. 3(a, b). The NH_4^+–N concentrations in the pre-anoxic zone, anaerobic zone, anoxic zone, and aerobic zone were 5.8, 11.9, 6.7, 1.6 mg L^{-1} (phase I) and 6.5, 11.3, 7.6, 1.7 mg L^{-1} (phase II), respectively. Meanwhile, the NO_3^-–N concentration in each zone was 5.6, 0.6, 5.5, 11.5 mg L^{-1} (phase I) and 5.9, 1.2, 5.9, 11.9 mg L^{-1} (phase II), respectively. The TN removal efficiency of the JHB process was 52.5 % (phase I) and 53.3 % (phase II; Fig. 2(c)). However, it was noticed that the promotion of NO_3^-–N removal by step-feed technology was inconspicuous in phase II. This was caused by insufficient influent COD and DO brought to the anoxic zone by nitrate recycling. Due to an electron donor shortage, NO_3^-–N represented a major proportion of effluent TN in the JHB process. Therefore, the SAD process was proposed to further improve NO_3^-–N removal. For the SAD process, the influent concentrations of TN and NO_3^-–N in phase I were 13.8 mg L^{-1} and 11.6 mg L^{-1}, respectively. The SAD effluent concentrations of TN and NO_3^-–N were reduced to 1.4 and 0.8 mg L^{-1}, respectively, with the TN removal efficiency of the JHB-SAD system reaching 95.1%. During phase II, limestone and dolomite were added separately to regulate the pH in the SAD reactors. Fig. 2(c) shows that the removal performance of NO_3^-–N was analogous to SAD S1#, although part of the sulfur was replaced by limestone or dolomite. Thus, sulfur would supply enough electrons for autotrophic denitrification in the SAD process. The removal rate of NO_3^-–N may rely on the activity of sulfur autotrophic denitrifying bacteria. Meanwhile, the effluent NO_3^-–N in SAD S1#–S4# decreased from 8.7 mg L^{-1} to 2.6 mg L^{-1} after 7 days of acclimation in phase II, which indicated that the start-up process of the SAD reactor was a saving-time process. Moreover, the SAD process obtained a short AHRT compared to that in the previous reports [24,25]. This could be primarily attributed to two aspects. First, the nitrate concentration of the SAD reactors influent was averagely maintained at 11.6 mg L^{-1} (phase I) and 11.9 mg L^{-1} (phase II) which was lower than the previous reports [6,24,25]. Second, nitrite, which is harmful to microorganisms, was not accumulated in the SAD process. The results suggested that the nitrogen removal performance was obviously improved, and the TN removal efficiency reached 95.1% with an influent COD/TN ratio of 4–5 when the SAD process was applied. In the JHB-SAD system, the JHB process was used for maximum nitrogen removal by utilizing influent organic carbon, and then, SAD utilized sulfur as an electron donor for autotrophic denitrification to enhance nitrate removal. Thus, the JHB-SAD system was beneficial for nitrogen removal from wastewater with a low COD/TN ratio. Nitrogen could be almost completely removed by the JHB-SAD system if the NH_4^+–N was sufficiently oxidized. The nitrogen removal performance of the JHB-SAD system is attractive compared with other low COD/TN ratio nitrogen removal processes (Table 1).

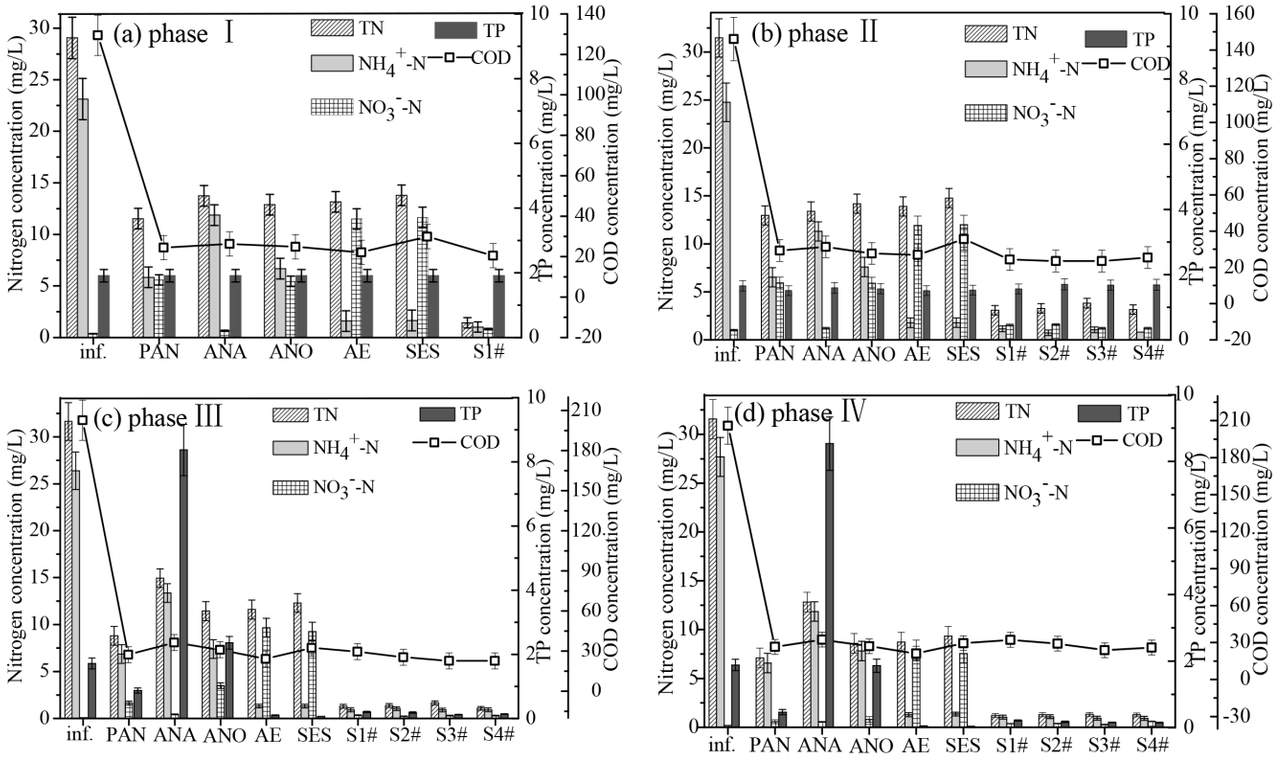

Fig. 3. Variations of COD, NH4+-N, TN NO3--N and TP in each zone of the JHB-SAD system at different phases. (a) phase I; (b) phase II; (c) phase III; (d) phase IV. PAN: pre-anoxic zone; ANA: anaerobic zone; ANO: anoxic zone; AE: aerobic zone; SES: secondary settler; S1#–S4#: sulfur autotrophic denitrification reactor (SAD) 1#–4#.

Table 1
Comparison of the documented efficiency of other low COD/TN ratio nutrient removal processes

Waste water source	Influent COD (mg L^{-1})	Influent TN (mg L^{-1})	Influent TP (mg L^{-1})	COD/TN ratio	Wastewater treatment process	Effluent COD (mg L^{-1})	Effluent TN (mg L^{-1})	Effluent TP (mg L^{-1})	Removal efficiency of TN (%)	Removal efficiency of TP (%)	References
Municipal waste water	295 on average	58.5 on average	4.57	5–6	Modified UCT step feed	43.5 ± 6.5	11.6 ± 2.7	<0.5	85–90	>90	[26]
Municipal waste water	160 ± 310	31.73 ± 3.66	31.73 ± 3.66	5.16 ± 0.83	Modified four step-feed	33.0	9.26	<0.46	70.24	86.7	[27]
Campus waste water	177.5 with NaAc (COD of 50 mg L^{-1})	73.7 on average	5.17	1.84–3.85	A^2O	<50	9.2	0.21	85	96	[28]
Campus waste water	222	61	3.88	3.63	PITSF	26.0	9	0.18	86.86	95.4	[29]
Municipal waste water	387.2	73.3	5.8	5.28	A2O-BAF	39.3	9.5	−0.1	87.0	98.3	[30]
Municipal waste water	129.4	29.1	1.70	4.45 on average	JHB-SAD	20.5	1.42	1.77	95.1		This study phase I
Municipal waste water	146.1	31.5	1.67	4.64 on average	JHB-SAD	22.9	3.15	1.69	90.0		This study phase II
Municipal waste water	152.7 with NaAc (COD of 40 mg L^{-1})	31.6	1.72	5.0–6.5	JHB-SAD	22.7–29.5	1.4	0.17	95.2	90.1	This study phase III
Municipal waste water	155.9 with NaAc (COD of 40 mg L^{-1})	31.6	1.88	– 5.0–6.5	JHB-SAD	22.7–32.2	1.28	0.17	95.9	91.0	This study phase IV

The TP removal performance of JHB-SAD is shown in Fig. 2(d) and Fig. 3. During phases I–II, the average influent TP concentrations were 1.70 mg L^{-1} and 1.67 mg L^{-1}, respectively, with corresponding effluent concentrations of 1.73 mg L^{-1} and 1.67 mg L^{-1} on average. The results indicated that the JHB-SAD system would not significantly enhance the removal performance of TP with the influent of a low COD/TN ratio. Although there was an anaerobic zone in the JHB process, phosphorus release could not be accomplished (Fig. 3(a, b)). Insufficient influent COD prevented PAOs from obtaining enough organic carbon for phosphorus release. Furthermore, NO_3^-–N (approximately 6 mg L^{-1}) from the pre-anoxic zone entered the anaerobic zone, which resulted in competition between denitrifying heterotrophs and PAOs for organic carbon.

3.1.2. Pollutant removal in the JHB-SAD system with added sodium acetate

Although the TN removal performance was excellent in phase I and phase II, the TP removal performance of the JHB-SAD system was insufficient due to the shortage of organic carbon. Therefore, sodium acetate (COD of 40 mg L^{-1}) was added to enhance the TP removal performance in phase III and phase IV.

During phase III–IV, the effluent concentrations of COD and NH_4^+–N in the JHB-SAD system were 26.1 mg L^{-1} and 1.29 mg L^{-1} on average, respectively, with corresponding removal efficiencies of 87.2 and 95.2%, as shown in Fig. 2(a, b). The COD was effectively removed before inflowing into the aerobic zone, even though the influent COD was increased by adding sodium acetate. Meanwhile, the JHB process maintained excellent NH_4^+–N removal performance. However, Fig. 2 shows that the SAD effluent concentrations of COD were approximately 2–10 mg L^{-1} lower than the secondary settler effluent. The SAD S3# reactor effluent COD concentration was the lowest, which resulted in the filtration of sulfur granules and limestone. NH_4^+–N effluent concentrations were approximately 0.3–0.5 mg L^{-1}, which were lower than those in the JHB process effluent. This result was found because the assimilation of sulfur autotrophic bacteria and NH_4^+–N served as a nitrogen source. The results revealed that the COD and NH_4^+–N removal performances in phase III and phase IV were analogous to the performance from phase I to phase II.

The TN removal performances of the JHB-SAD system during phase III and phase IV are illustrated in Figs. 2 and 3. The influent TN content was approximately 31.6 mg L^{-1} and was primarily composed of NH_4^+–N (86.1%). The JHB process effluent TN and NO_3^-–N contents were 12.3 mg L^{-1} and 9.3 mg L^{-1} (phase III) and 9.3 mg L^{-1} and 7.6 mg L^{-1} (phase IV), respectively. Compared to phase I and phase II, the TN removal performances of the JHB process were improved by adding sodium acetate (COD of approximately 40 mg L^{-1}). The corresponding TN removal efficiencies of the JHB process were increased from 52.5 % (phase I) and 53.0 % (phase II) to 62.7% (phase III) and 70.5% (phase IV). Principally, the NO_3^-–N concentrations in the pre-anoxic zone were 1.64 mg L^{-1} and 0.57 mg L^{-1} in phase III and phase IV, respectively. Compared to phase I and phase II, the NO_3^-–N concentration was obviously decreased before inflowing into the anaerobic zone, which was favorable for PAOs to release phosphorus. Moreover, the denitrification was enhanced by step-feed technology, and the NO_3^-–N concentration in the anoxic zone was decreased from 3.5 mg L^{-1} (phase III) to 0.8 mg L^{-1} (phase IV), with 30% influent flowing into the anoxic zone. To further enhance the nitrogen removal performance, the SAD process was used to remove NO_3^-–N from the JHB process effluent during phase III and phase IV. The TN and NO_3^-–N concentrations in SAD reactors' effluent were 1.09–1.66 and 0.22–0.59 mg L^{-1}, respectively. The results revealed that the TN removal performances were analogous among the SAD S1#–S4# reactors at the same AHRT of 10 min. When the SAD process was applied to wastewater treatment, it was recommended to add limestone or dolomite to the SAD reactor because either of these additives could neutralize the H^+ produced in the SAD process. The nitrogen removal rate of SAD was quite fast (SAD AHRT of 10 min), which means that the SAD process was space-saving. When it was not necessary to completely remove the nitrogen pollutant, WWTPs only needed to treat part of the JHB effluent via the SAD process, and then, the untreated JHB process effluent and the SAD process effluent were mixed to control the nitrogen pollutant concentration at an acceptable level. In addition, the step-feed ratio of the anaerobic zone can be increased appropriately for the phosphorus release process because nitrate removal could be enhanced by SAD process, which may present a solution to the problem of denitrifying heterotrophs and PAOs competing for organic carbon.

During phase III–IV, the TP removal performance was obviously improved by adding sodium acetate. Fig. 2(d) shows that the influent TP concentrations were 1.72 mg L^{-1} and 1.88 mg L^{-1} on average. The TP contents in JHB process effluent were 0.07 mg L^{-1} and 0.05 mg L^{-1} with corresponding removal efficiencies of 95.7 and 97.2%. Fig. 3(c, d) show that the TP concentrations in the pre-anoxic zone, anaerobic zone, anoxic zone, and aerobic zone were 1.11, 8.38, 2.87, 0.11 mg L^{-1} (phase III) and 0.47, 8.53, 1.86, 0.04 mg L^{-1} (phase IV), respectively. The results revealed that the phosphorus release process occurred in the anaerobic zone. This was because the NO_3^-–N concentration was sufficiently low and was not an inhibition factor of phosphorus release in the anaerobic zone. Meanwhile, sodium acetate is a volatile fatty acid and a product of fermentable COD, which was utilized by PAOs to generate polyhydroxyalkanoates (PHA). Supposing that there was excessive NO_3^-–N in the anaerobic zone, denitrifying heterotrophs would compete with PAOs for organic carbon, and net phosphorus release would not occur until completion of the denitrification process [11]. However, the TP effluent concentration of the SAD process (approximately 0.14–0.21 mg L^{-1}) was higher than that of the JHB process effluent. This was because phosphorus was the second compound to be released in the anoxic environment of the SAD process. Fig. 2 shows that the JHB-SAD system effluent concentration of COD, TN and TP was 27.1, 1.28 and 0.18 mg L^{-1} on average during phases III–IV, respectively. The results suggested that the JHB-SAD system with added sodium acetate (COD of 40 mg L^{-1}) successfully achieved efficient nutrients removal when treating municipal wastewater with a low COD/TN ratio (COD 146.7 mg L^{-1}, TN 31.5 mg L^{-1} and TP 1.79 mg L^{-1}). The nutrients removal performance of the JHB-SAD system is attractive compared with other low COD/TN ratio nutrients removal processes (Table 1).

3.1.3. Changes in pH and SO_4^{2-}

The changes in pH and SO_4^{2-} throughout the JHB-SAD system were investigated and are shown in Fig. 4. The influent pH was approximately 7.35–7.50 (phases I–II) and slightly increased in phase III and phase IV (approximately 7.64–7.75), due to the hydrolytic equilibrium of sodium acetate.

During phases I–IV, the pH values in the pre-anoxic zone were 7.20, 7.05, 7.74 and 7.85. Compared with the influent, the pH values in the pre-anoxic zone decreased in phases I–II but increased in phases III–IV. This was because the denitrification process was enhanced by adding sodium acetate in the pre-anoxic zone. Compared to the pre-anoxic zone, the pH in the anaerobic zone increased to 7.32 (phase I) and 7.15 (phase II). Due to the shortage of organic carbon in phases I–II, nitrate in sludge return could not be completely removed in the pre-anoxic zone. The denitrification process continuously removed residual nitrate while producing OH^- in the anaerobic zone. In contrast, the pH decreased to 7.71 and 7.77 from the pre-anoxic zone to the anaerobic zone in phase III and phase IV because nitrate was completely removed in the pre-anoxic zone, and phosphorus released with the production of H^+ played a dominant role in the anaerobic zone, as shown in Fig. 3(c, d). In summary, different biochemical reactions that occurred in the anaerobic zone led to different pH responses. The pH initially increased in the anoxic zone then decreased in the aerobic zone during phases I–IV because denitrification and nitrification were the primary biochemical reactions in the anoxic zone and aerobic zone, respectively.

Because of the H^+ produced by the SAD process, limestone and dolomite were added to the SAD S2#–S4# reactors with granular sulfur. Fig. 4(a) shows that the pH values of S1#–S4# were 6.70, 6.83, 6.98 and 6.84 in phase II, respectively. Afterwards, SAD influent pH values in phase III and phase IV were higher than those in phase II. This indicated that more OH^- was utilized to neutralize the H^+ produced by the SAD process in phases III–IV, which decreased the effect of limestone and dolomite on the pH values, as shown in Fig. 4(a). The result indicates that limestone and dolomite could appropriately increase the pH values. However, the difference in pH among SAD reactors S1#-S4# was very small, which could be attributed to three aspects. First, the AHRT of the SAD process was short; thus, the neutralization effect of limestone and dolomite was not obvious. Second, the additive amount of limestone and dolomite is small. Third, the neutralization effect of limestone and dolomite was reduced when the pH value was high. On the other hand, nitrogen removal performance was almost not affected by H^+ produced during the SAD process. The reasons were attributed to three aspects. First, the nitrate concentration was relatively low (7–12 mg L^{-1} in phase I-IV) in the SAD influent, so the amount of H^+ produced was relatively small. Second, the total alkalinity in the wastewater was high compared to surface water and groundwater, which alleviated the negative effect of H^+ on the SAD process. The total alkalinity was among 123–155 mg L^{-1} ($CaCO_3$) in SAD influent, and then that was decreased to 75–117 mg L^{-1} ($CaCO_3$) in SAD reactors effluent. Third, the pH values of SAD reactors effluent were all above 6.5, which almost not affect the nitrogen removal efficiency of SAD process [31].

The change in SO_4^{2-} concentration throughout the JHB-SAD system is presented in Fig. 4(b). The SO_4^{2-} concentration varied between 65.7 and 93.0 mg L^{-1} throughout the JHB process during phase I–phase IV. The effluent SO_4^{2-} concentration was increased when SAD was applied to enhance nitrate removal. The SO_4^{2-} concentration in the JHB-SAD system effluent was approximately 129.8–178.4 mg L^{-1}. Because sulfur served as an electron donor in the SAD process, as more nitrate was removed by the SAD process, more SO_4^{2-} was produced. The average ratio of SO_4^{2-} production to NO_3^-–N removal was 7.54, which was similar to the value in another report [32]. The change of NO_2^-–N in the SAD process was slight, and the concentration was maintained at 0.02–0.05 mg L^{-1}. Therefore, SO_4^{2-} production was barely affected by nitrite variation in this study.

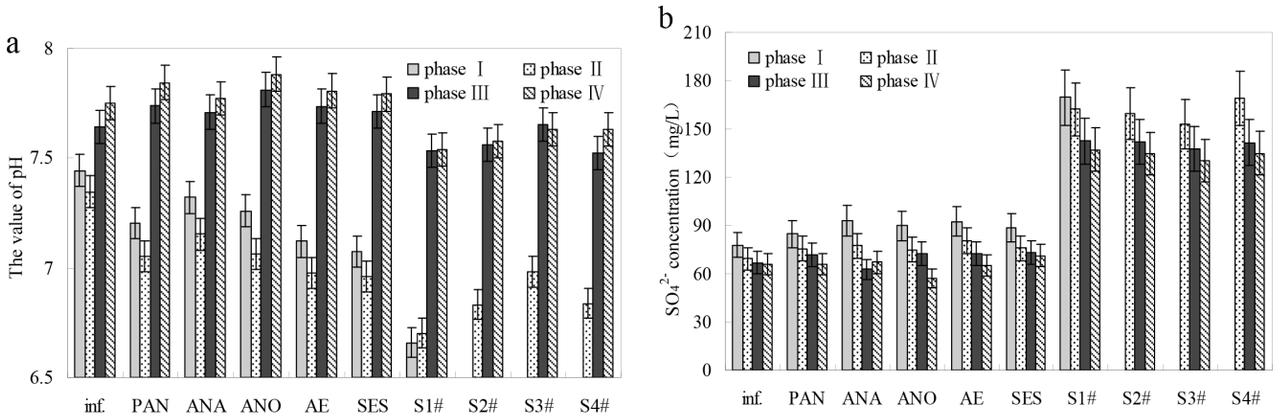

Fig. 4. Variations of (a) pH and (b) SO42-- in each zone of the JHB-SAD system during phase I -phase IV. PAN: pre-anoxic zone; ANA: anaerobic zone; ANO: anoxic zone; AE: aerobic zone; SES: secondary settler; S1#-S4#: sulfur autotrophic denitrification reactor (SAD) 1#-4#.

3.2. Material balance and pollutant removal mechanisms in the JHB-SAD system

3.2.1. COD removal

The COD and nutrients utilization performances of the JHB-SAD system during phases I–IV are shown in Fig. 5. This figure reveals that the COD removal efficiencies of the non-aerobic zone in the JHB process were 84.0, 88.1, 78.7 and 82.3%, and the removal efficiencies of the aerobic zone were 8.5, 2.2, 13.5 and 11.6% during phases I–IV, respectively. The COD concentration in the secondary settler effluent increased from 22–29 mg L^{-1} to 30–36 mg L^{-1}, due to the suspended solid and activated sludge outflow; however, 2–10 mg L^{-1} COD was removed by the filtration of sulfur granules in the SAD process. The results indicated that COD was effectively consumed when the influent flowed into the JHB-SAD system. This was because COD was utilized by the denitrification process in the pre-anoxic and anoxic zones to remove nitrate and was assimilated by PAOs in the anaerobic zone for phosphorus release. The capacity of COD removal in the aerobic zone was small because the COD concentration remained at a low level when the mixture flowed into the aerobic zone. This could explain why the COD did not substantially change much in the JHB-SAD system effluent, although the influent COD fluctuated in the range of 100–250 mg L^{-1} during phases I–IV.

3.2.2. Nitrogen removal

Fig. 5 shows that the capacity of NH_4^+–N removal in the aerobic zone was 272.6 g d^{-1}, 312.1 g d^{-1}, 336.8 g d^{-1} and 351.1 g L^{-1} with corresponding removal efficiencies of 87.8, 93.8, 95.0 and 94.3% during phases I–IV, respectively. These results indicated that NH_4^+–N was mainly removed by the nitrification process in the aerobic zone with nitrate formation. The outstanding NH_4^+–N removal obtained by the JHB-SAD system could be primarily attributed to two aspects. First, COD was effectively consumed before flowing into the aerobic zone, which would benefit the metabolism of nitrifying bacteria and avoid the inhibitory effect caused by the excessive COD. Second, the SRT of the JHB process was controlled at 27–33 d (phases I–II) and 17–23 d (phases III–IV), which benefited the enrichment of the nitrifying bacteria.

During phases I–II, TN was mainly removed by the denitrification process in the pre-anoxic zone, anaerobic zone and SAD reactors, as shown in Fig. 5. The capacities of TN removal in the pre-anoxic zone, anaerobic zone and SAD reactors were 101.1 g d^{-1} (25.9%), 105.5 g d^{-1} (27.0%), and 166.2 g d^{-1} (42.6%) in phase I and 98.9 g d^{-1} (23.4%), 89.8 g d^{-1} (21.2%), and 153.7 g d^{-1} (36.4%) in phase II. Due to the shortage of organic carbon, heterotrophic denitrification could not effectively remove the nitrate carried by return sludge in the pre-anoxic zone, and the residual nitrate was removed in the anaerobic zone. Subsequently, only 7.8% (phase I) and 10.3% (phase II) TN removal was obtained in the anoxic zone. The results showed that the nitrogen removal performance was ineffective in the anoxic zone because limited organic carbon was provided for the anoxic denitrification process in phase I, and 7.8% TN removal was attributed to endogenous respiration denitrification. However, 30% influent, which flowed into the anoxic zone in phase II, indistinctively improved

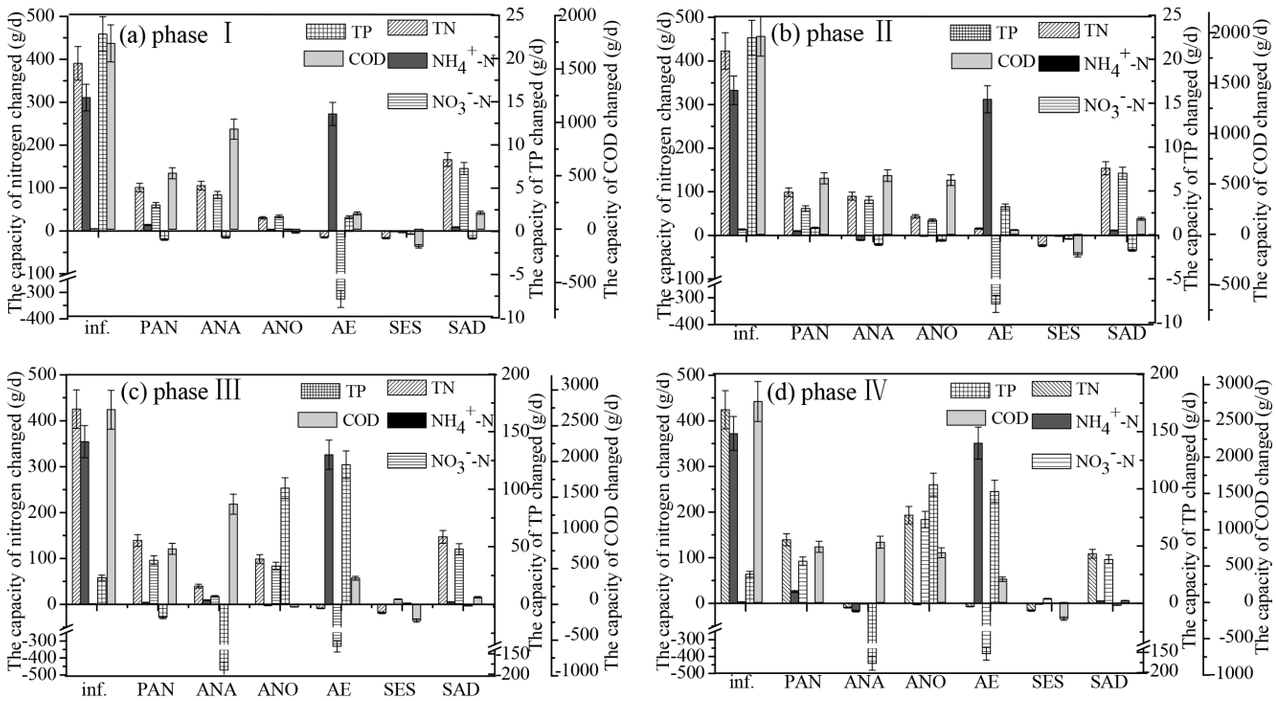

Fig. 5. Removal capacity of COD, NH4+-N, TN, NO3--N and TP in each zone of the JHB-SAD system at different phases. (a) phase I; (b) phase II; (c) phase III; (d) phase IV. PAN: pre-anoxic zone; ANA: anaerobic zone; ANO: anoxic zone; AE: aerobic zone; SES: secondary settler; SAD: sulfur autotrophic denitrification reactor.

nitrogen removal performance. This was because the DO brought to the anoxic zone by nitrate recycling would have consumed organic carbon prior to the denitrification process. In the aerobic zone, ammonia was converted into nitrate by nitrifying bacteria, and COD remained at a low level. Therefore, nitrate accounted for the major proportion of effluent TN in JHB effluent. Based on the characteristics of the effluent from the JHB process, the SAD process was proposed to further remove nitrate. In the SAD process, the average TN removal performance was 166.2 g d^{-1} (42.6%) and 153.7 g d^{-1} (36.4%) during phases I–II, respectively.

During phases III–IV, TN removal mainly took place in the pre-anoxic zone, anoxic zone and SAD reactors with added sodium acetate (COD of 40 mg L^{-1}) as shown in Fig. 5. The capacity of TN removal in the pre-anoxic zone, anoxic zone and SAD reactors was 139.2 g d^{-1} (32.7%), 98.6 g d^{-1} (23.2%) and 147.1 g d^{-1} (34.6%) in phase III and 128.6 g d^{-1} (30.3%), 192.8 g d^{-1} (45.4%) and 108.3 g d^{-1} (25.5%) in phase IV. It was notable that only 11.7% (phase III) and 0.2% (phase IV) TN contents were removed in the anaerobic zone because most of the nitrate carried by the sludge return was effectively removed in the pre-anoxic zone with the corresponding NO_3^-–N concentration of 1.64 mg L^{-1} (phase III) and 0.58 mg L^{-1} (phase IV). A low NO_3^-–N concentration in the pre-anoxic zone effluent was beneficial to phosphorus release in the anaerobic zone because NO_3^-–N could result in competition for organic carbon between denitrifying heterotrophs and PAOs. In phase III, nitrate and phosphorous were removed simultaneously with 23.2% TN removal in the anoxic zone, although organic carbon was not provided for denitrification by the influent. The TN removal performance of the anoxic zone in phase III was obviously higher than the 7.8% TN removal in the anoxic zone during phase I, which indicated that part of the nitrate was removed in the anoxic zone via denitrifying phosphorous removal. Based on step-feed technology, 30% influent flowed into the anoxic zone in phase IV, which increased the TN removal from 98.6 g d^{-1} (phase III) to 192.8 g d^{-1} (phase IV). This result indicates that improved TN removal was obtained by step-feed technology with added sodium acetate (COD of 40 mg L^{-1}). The improved TN removal obtained by the JHB-SAD system in phase IV was mainly attributed to two aspects. First, 30% influent flowed into the anoxic zone, which provided electron donors for the denitrification process and enhanced nitrate removal in the anoxic zone. Second, the effect of DO on denitrification efficiency, which was derived from nitrate recycling, was eliminated by higher influent COD concentration during phase IV. DO could have caused the consumption of organic carbon prior to the denitrification process, but surplus COD was utilized by denitrification in the anoxic zone. In the SAD reactors, nitrogen was further removed by the autotrophic denitrification process with the JHB-SAD effluent TN concentration of 1–2 mg L^{-1} during phases III–IV.

3.2.3. Phosphorous removal

In phases I–II, the phosphorous removal performance of the JHB-SAD system was inefficient. Although the anaerobic zone existed in the JHB process, phosphorous release did not occur due to a shortage of organic carbon and nitrate flowing into the anaerobic zone. In phases III–IV, the phosphorous removal performance was obviously improved by adding sodium acetate. The capacity of anaerobic phosphorus release was increased to 189.7 g d^{-1} and 176.7 g d^{-1}, accounting for 837.2 and 698.4% of influent TP, respectively. As shown in Fig. 3(c, d), the nitrate content was low in the anaerobic zone. Moreover, sodium acetate was added as external organic carbon. Therefore, PAOs can take full advantage of volatile fatty acid from the influent to synthesize PHAs and to release phosphorus. It is notable that 101.0 g d^{-1} (phase III) and 97.8 g d^{-1} (phase IV) phosphorus was removed in the anoxic zone, which is associated with denitrifying phosphorus removal. Afterwards, 121.3 g d^{-1} and 97.8 g d^{-1} phosphorus was further removed in the aerobic zone during phases III–IV.

3.3. Bacterial community

3.3.1. Richness and diversity of bacterial communities

The numbers of OTUs, coverage percentage, ACE, Chao1 and Shannon indices were calculated for the sludge samples of the JHB-SAD system (Table 2). The results showed that the Good's coverage of the five sludge samples ranged from 73.0 to 88.1%, indicating that the sequence libraries constructed in this study could cover the diversity of the bacteria community. The OTU numbers were 5716 (pre-anoxic zone), 5936 (anaerobic zone), 5608 (anoxic zone), 4268 (aerobic zone) and 4694 (SAD reactor S3#), which were consistent with those in a previous report [33] but were higher than those found by Zhang et al. [21]. The patterns of Chao1 and the ACE values in the anaerobic zone sludge sample were the largest, and the richness values varied by 2–3 times among the five samples. These results demonstrated that the pre-anoxic, anaerobic and aerobic zones displayed higher bacterial diversity than did the aerobic zone and the SAD reactor, which could be mainly attributed to two factors. First, bacterial communities were diverse in the influent, and the most dominant bacteria were different from activated sludge [33], indicating that a variety of bacteria were imported via the influent and resulted in higher

Table 2
Richness and diversity estimators of the microbial community in the JHB-SAD system

Samples	OTU	Good's coverage	Chao 1	ACE	Shannon
PAN	5716	0.840	16837	29755	7.19
ANA	5936	0.730	21747	45271	7.52
ANO	5608	0.857	15556	26245	7.13
AE	4268	0.881	10776	17416	6.91
SAD	4694	0.861	11288	17771	7.03

bacterial diversity in the pre-anoxic, anaerobic and anoxic zones than in the aerobic zone and SAD reactor S3#. Second, more diverse biochemical reactions were performed in the pre-anoxic, anaerobic and anoxic zones, such as fermentation, heterotrophic denitrification and anaerobic phosphorus release. In contrast, nitrification and phosphorus uptake processes were mainly conducted in the aerobic zone and autotrophic denitrification in the SAD process as discussed in section 3.2. The higher diversity of bacterial communities in the pre-anoxic, anaerobic and anoxic zones could be due to the diversity of the primary biochemical reactions.

3.3.2. Bacterial taxonomic identification

To evaluate the bacterial construction of the JHB-SAD system, the effective bacterial sequences in each sample were assigned to different taxa levels (from phylum to genera) by the RDP Classifier at an 80% threshold. At the phylum level, 25 phyla were detected in five sludge samples, with 8 dominating phyla (>1% abundance in any sludge sample from the JHB-SAD system) (Fig. 6(a)). These 8 phyla accounted for 86.8–91.1% of the total effective bacterial sequences: *Proteobacteria* (34.7–57.5%), *Bacteroidetes* (11.7–23.4%), *Planctomycetes* (8.71–20.1%), *Chloroflexi* (3.08–9.42%), *Firmicutes* (1.83–3.00%), *Verrucomicrobia* (0.41–1.81%), *Gemmatimonadetes* (0.44–1.27%) and *Chlorobi* (0.30–1.05%). These were similar to the major phyla reported in previously studies [20,21]. The majority of these phyla, particularly *Proteobacteria* and *Bacteroidetes*, are ubiquitous and widely exist in WWTPs and wastewater; however, their relative abundances were different in various environments. For example, the abundance of *Planctomycetes* was higher in this study than in previous reports [20,33]. In addition, the abundance of *Verrucomicrobia* in the JHB process was higher than that in the SAD reactor, whereas the abundances of *Gemmatimonadetes* and *Chloroflexi* in the SAD reactor were obviously higher than those in the JHB process.

At the class level, 53 bacterial classes were detected in the five sludge samples. The 17 dominant classes (>1% in at least one sample) accounted for 85.8–90.2% of the total effective bacterial sequences, as shown in Fig. 6(b). Among the 17 classes, *Alphaproteobacteria*, *Betaproteobacteria*, *Gammaproteobacteria*, *Deltaproteobacteria*, *Anaerolineae*, *Sphingobacteriia*, *Flavobacteriia* and *Planctomycetacia* were commonly shared by all five sludge samples from the JHB-SAD system. The other 5 classes with at least a 1% abundance appeared in two or more zones of the JHB-SAD system, including *Caldilineae, Bacilli, Verrucomicrobiae, Clostridia* and *Phycisphaerae*. A few classes, including *Gemmatimonadetes, Epsilonproteobacteria, Ignavibacteria* and *Cytophagia*, were the major (abundance >1%) classes in only one unit of the JHB-SAD system. *Sphingobacteriia* was the most abundant class (8.56–20.4%, averaging 16.0%) in the JHB-SAD system, and the abundance of *Sphingobacteriia* in the JHB process (averaging 17.9%) was higher than that in the SAD reactor (8.56%). Within *Proteobacteria*, *Alphaproteobacteria* was the most dominant class in the aerobic zone. In the anaerobic zone and SAD reactor, *Betaproteobacteria* was the most dominant *Proteobacteria*, and *Gammaproteobacteria* was the most abundant *Proteobacteria* in the pre-anoxic and anoxic zones. This result indicates that the most abundant class within *Proteobacteria* was different in units of the JHB-SAD system, even in the same wastewater treatment process. Previous studies [21,33] reported that the most abundant class of *Proteobacteria* was not only different in various WWTPs but also different in the influent, active sludge and effluent of the same WWTP.

At the order level, 110 bacterial orders were identified in the JHB-SAD system, 24 of which were dominant (>1% in at least one sample), as shown in Fig. 6(c). The 24 abundant orders accounted for 80.6–84.2% of the total effective bacterial sequences. Among them, *Burkholderiales*, *Rhizobiales*, *Anaerolineales*, *Flavobacteriales*, *Rhodocyclales*, *Xanthomonadales*, *Pseudomonadales*, *Sphingobacteriales*, *Myxococcale* and *Planctomycetales* were the orders commonly shared by all five sludge samples. However, *Sphingobacteriales*, *Planctomycetales* and *Chromatiales* were significantly more abundant in the JHB process, whereas *Anaerolineales*, *Rhodocyclales*, *Hydrogenophilales*, and *Desulfobacterales* were more abundant in the SAD reactor. In addition, *Pseudomonadales* was more abundant in the pre-anoxic zone.

At the family level, 210 bacterial families were detected in the five sludge samples, and 26 abundant families (>1% in any of the five sludge samples) accounted for 73.6–78.7% of the total effective bacterial sequences, as shown in Fig. 6(d). Based on the analysis, *Moraxellaceae, Comamonadaceae, Chitinophagaceae, Planctomycetaceae, Saprospiraceae, Rhodocyclaceae, Anaerolineaceae, Hyphomicrobiaceae,* and *Xanthomonadaceae* were shared by all five sludge samples, whereas the other 17 families appeared in one or more units of the JHB-SAD system. Among the 26 dominant families, *Planctomycetaceae, Saprospiraceae, Chromatiaceae,* and *Verrucomicrobiaceae* were more abundant in the JHB process, whereas *Rhodocyclaceae, Anaerolineaceae Desulfobulbaceae* and *Xanthomonadaceae* were more abundant in the SAD reactor, and *Moraxellaceae* was more abundant in the pre-anoxic zone.

A total of 619 genera were identified in the JHB-SAD system, 129 of which were shared by all five sludge samples, accounting for 46.4–53.0% of total effective bacterial sequences. Among these 619 assigned genera, 47 abundant genera (>0.5% in any of the five sludge samples) accounted for 38.3–48.0% of the total sequences, and 20 abundant genera (>1% in any of the five sludge samples) accounted for 28.4–35.5% of the total sequences. The 20 abundant genera were selected and compared with their abundances in other samples as shown in Fig. 6(e). Among the 20 selected genera, *Acidovorax, Planctomyces, Azospira* and *Acinetobacter* were abundant in all five sludge samples, and *Solitalea, Methylocystis, Gemmata* and *Hyphomicrobium* were commonly shared by the JHB process, whereas *Ferritrophicum, Thiobacillus, Desulfocapsa, Hyalangium* and *Sulfuritalea* were more abundant in the SAD reactor.

3.3.3. Relationships between pollutant removal and community structure

RDA analysis was used to reveal the relationship between the abundance of bacterial phyla and pollutant

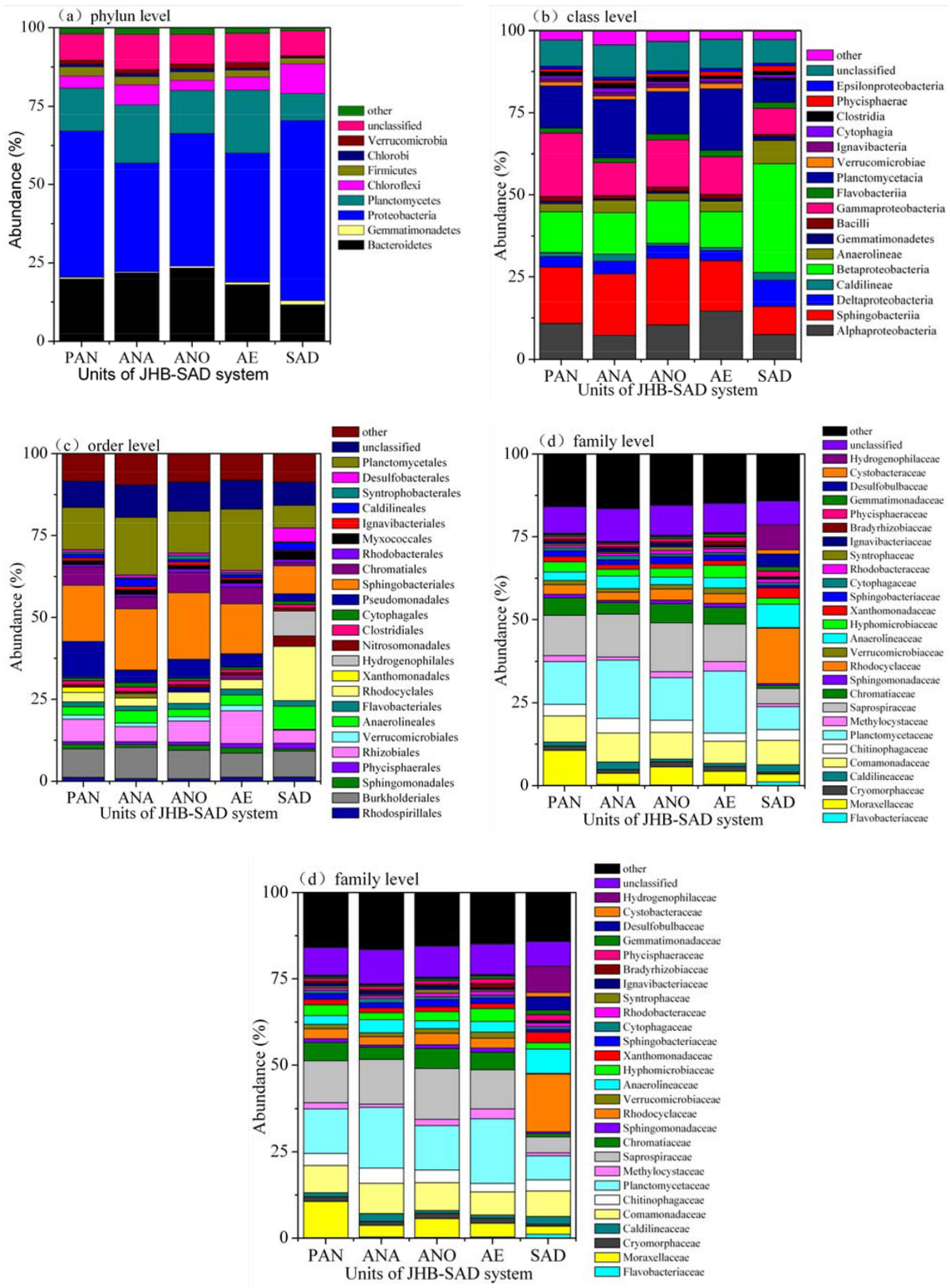

Fig. 6. Distributions of bacteria in the JHB-SAD system at the (a) phylum level, (b) class level, (c) order level, and (d) family level and (e) heat map of the 20 most abundant genera. Taxa represented occurrence at >1% frequency in at least one sample. PAN: pre-anoxic zone; ANA: anaerobic zone; ANO: anoxic zone; AE: aerobic zone; SAD: sulfur autotrophic denitrification reactor.

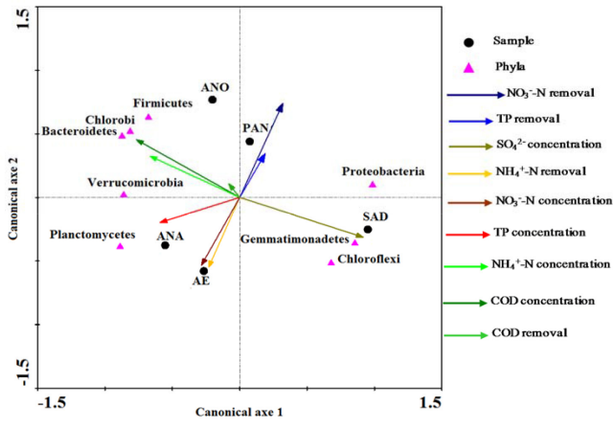

Fig. 7. Redundancy Analysis (RDA) to investigate the ecological correlation between the abundance of phylum and environmental parameters. PAN: pre-anoxic zone; ANA: anaerobic zone; ANO: anoxic zone; AE: aerobic zone; SAD: sulfur autotrophic denitrification reactor.

removal as shown in Fig. 7. The first and second canonical axes were 11.1 and 84.1% of variation, respectively. The triplet analysis showed that the phyla *Bacteroidetes*, *Chlorobi*, and *Firmicutes* were related to COD, NH_4^+–N concentration and COD removal, and the phyla *Gemmatimonadetes* and *Chloroflexi* were related to SO_4^{2-} concentration in the SAD reactor due to autotrophic denitrification. Because of the anaerobic phosphorus release, the TP concentration positively responded to the anaerobic zone, whereas NH_4^+–N removal and NO_3^-–N concentration were positively correlated with the aerobic zone due to nitrification. NO_3^-–N removal was passively correlated with the aerobic zone, and nitrogen pollutant removal was achieved in the pre-anoxic zone, anoxic zone and SAD reactor according to the RDA analysis and the material balance calculation. In addition, TP removal had a mixed correlation with anaerobic phosphorus release and phosphorus uptake in the anoxic and aerobic zones according to the material balance calculation and RDA analysis. By comparing the positive relationship between TP removal and phosphorus uptake in the anoxic and aerobic zones, anaerobic phosphorus release had a more negative effect on TP removal.

4. Conclusions

This study explored a novel and efficient nutrients removal technology that integrated the JHB process and the SAD process. The result demonstrated that the JHB-SAD system achieved efficient removal of nitrogen and carbon pollutants when treating municipal wastewater with a low COD/TN ratio. Furthermore, the phosphorus removal performance of the JHB-SAD system improved with the addition of sodium acetate (COD of 40 mg L^{-1}). Most importantly, the JHB-SAD system can almost completely remove nitrogen if NH_4^+–N is sufficiently oxidized. Additional, it was found that the phyla *Proteobacteria*, *Bacteroidetes*, *Planctomycetes*, *Chloroflexi*, *Firmicutes*, *Verrucomicrobia*, *Gemmatimonadetes* and *Chlorobi* constituted the majority of the bacteria in the JHB-SAD system.

Acknowledgements

This work was financially supported by the Major Science and Technology Program for Water Pollution Control and Treatment of China (2012ZX07202-005 & 2013ZX07202-010). We would like to thank Doctor Jianli Liu for her assistance in high-throughput sequencing, and we would like to thank Factory director Rong Zhao and Engineer Tao Zheng for their assistance providing the experimental sites.

Symbols

Q_{PAN}, Q_{ANA} and Q_{ANO} — the influent flows of the pre-anoxic, anaerobic and anoxic zones, respectively;

Q_R and Q_r — the nitrate recycling flow and sludge return flow, respectively;

$C_{inf.C,N,P}$, $C_{PAN.C,N,P}$, $C_{ANA.C,N,P}$, $C_{ANO.C,N,P}$, $C_{SES.C,N,P}$ $C_{SAD.C,N,P}$ and — pollutant concentrations in the influent, pre-anoxic zone, anaerobic zone, anoxic zone, aerobic zone, secondary settler and SAD reactor, respectively;

$\Delta S_{PAN.C,N,P}$, $\Delta S_{ANA.C,N,P}$, $\Delta S_{ANO.C,N,P}$, $\Delta S_{AE.C.N,P}$, $\Delta S_{SES.C,N,P}$ and $\Delta S_{SAD.C,N,P}$ — the capacity of pollutants changed in the pre-anoxic zone, anaerobic zone, anoxic zone, aerobic zone, secondary settler and SAD reactor, respectively.

References

[1] Y. Zhang, X.C. Wang, Y. Ge, M. Dzakpasu, Y. Zhao, J. Xiong, Effects of annual harvesting on plants growth and nutrients removal in surface-flow constructed wetlands in northwestern China, Ecol. Eng., 83 (2015) 268–275.
[2] K. Show, D. Lee, X. Pan, Simultaneous biological removal of nitrogen–sulfur–carbon: Recent advances and challenge, Biotechnol. Adv., 31 (2013) 409–420.
[3] J. Huang, J. Xu, X. Liu, J. Liu, L. Wang, Spatial distribution pattern analysis of groundwater nitrate nitrogen pollution in Shandong intensive farming regions of China using neural network method, Math. Comput. Model., 54 (2011) 995–1004.
[4] G.T. Frumin, and I.M. Gildeeva, Eutrophication of water bodies-A global environmental problem, Russ. J. Gen. Chem., 84 (2015) 2483–2488.
[5] I. García-Garizábal, J. Causapé, R. Abrahao, Nitrate contamination and its relationship with flood irrigation management, J. Hydrol., 442–443 (2012) 15–22.
[6] Y. Sun, and M. Nemati, Evaluation of sulfur-based autotrophic denitrification and denitritation for biological removal of nitrate and nitrite from contaminated waters, Bioresour. Technol., 114 (2012) 207–216.
[7] T. Khin, and A.P. Annachhatre, Novel microbial nitrogen removal processes. Biotechnol. Adv., 22 (2004) 519–532.
[8] A. Oehmen, P.C. Lemos, G. Carvalho, Z. Yuan, J. Keller, L.L. Blackall, M.A.M. Reis, Advances in enhanced biological phosphorus removal: From micro to macro scale, Water Res., 41 (2007) 2271–2300.
[9] J. Ahn, T. Daidou, S. Tsuneda, A. Hirata, Characterization of denitrifying phosphate-accumulating organisms cultivated under different electron acceptor conditions using polymerase chain reaction-denaturing gradient gel electrophoresis assay, Water Res., 36 (2002) 403–412.
[10] P.S. Barker, P.L. Dold, Denitrification behaviour in biological excess phosphorus removal activated sludge system, Water Res., 30 (1996) 769–780.
[11] M. Henze, M.C.M. Van Loosdrecht, G.A. Ekama, D. Brdjanovic, Biological wastewater treatment: principles, modelling and design, IWA Publishing, London, 2008.
[12] J. Claros, J. Serralta, A. Seco, J. Ferrer, D. Aguado, Real-time control strategy for nitrogen removal via nitrite in a SHARON

reactor using pH and ORP sensors, Process Biochem., 47 (2012) 1510–1515.
[13] A. Gali, J. Dosta, M.C.M. Van Loosdrecht, J. Mata-Alvarez, Two ways to achieve an anammox influent from real reject water treatment at lab-scale: Partial SBR nitrification and SHARON process, Process Biochem., 42 (2007) 715–720.
[14] D. Gao, Y. Peng, B. Li, H. Liang, Shortcut nitrification–denitrification by real-time control strategies, Bioresour. Technol., 100 (2009) 2298–2300.
[15] X. Zhang, D. Zhang, Q. He, H. Ai, P. Lu, Shortcut nitrification–denitrification in a sequencing batch reactor by controlling aeration duration based on hydrogen ion production rate online monitoring, Environm. Technol., 35 (2014) 1478–1483.
[16] J. Yang, J. Trela, M. Zubrowska-Sudol, E. Plaza, Intermittent aeration in one-stage partial nitritation/anammox process. Ecol. Eng., 75 (2015) 413–420.
[17] H. Chen, S. Liu, F. Yang, Y. Xue, T. Wang, The development of simultaneous partial nitrification, ANAMMOX and denitrification (SNAD) process in a single reactor for nitrogen removal, Bioresour. Technol., 100 (2009) 1548–1554.
[18] S. Philips, S. Wyffels, R. Sprengers, W. Verstraete, Oxygen-limited autotrophic nitrification/denitrification by ammonia oxidisers enables upward motion towards more favourable conditions, Appl. Microbiol. Biotechnol., 59 (2002) 557–566.
[19] H. Li, B. Zhou, Z. Tian, Y. Song, L. Xiang, S. Wang, C. Sun, Efficient biological nitrogen removal by Johannesburg-Sulfur autotrophic denitrification from low COD/TN ratio municipal wastewater at low temperature, Environ. Earth Sci., 73 (2015) 5027–5035.
[20] D. Shu, Y. He, H. Yue, Q. Wang, Microbial structures and community functions of anaerobic sludge in six full-scale wastewater treatment plants as revealed by 454 high-throughput pyrosequencing, Bioresour. Technol., 186 (2015) 163–172.
[21] T. Zhang, M.F. Shao, L. Ye, 454 Pyrosequencing reveals bacterial diversity of activated sludge from 14 sewage treatment plants, ISME J., 6 (2012) 1137–1147.
[22] APHA, Standard methods for the examination of water and wastewater, 21st ed., American Public Health Association, USA, 2005.
[23] J. Gao, X. Luo, G. Wu, T. Li, Y. Peng, Abundance and diversity based on amoA genes of ammonia-oxidizing archaea and bacteria in ten wastewater treatment system, Appl. Microbiol. Biotechnol., 98 (2014) 3339–3354.
[24] H. Liu, W. Jiang, D. Wan, J Qu, Study of a combined heterotrophic and sulfur autotrophic denitrification technology for removal of nitrate in water, J. Hazard. Mater., 169 (2009) 23–28.
[25] D. Wan, H. Liu, J. Qu, P. Lei, S. Xiao, Y. Hou, Using the combined bioelectrochemical and sulfur autotrophic denitrification system for groundwater denitrification, Bioresour. Technol., 100 (2009) 142–148.
[26] Y. Peng, and S. Ge, Enhanced nutrient removal in three type of step feeding process from municipal wastewater, Bioresour. Technol., 102 (2011) 6405–6413.
[27] G. Cao, S. Wang, Y. Peng, Z. Miao, Biological nutrient removal by applying modified four step-feed technology to treat weak wastewater, Bioresour. Technol., 128 (2013) 604–611.
[28] W. Zeng, L. Li, Y. Yang, X. Wang, Y. Peng, Denitrifying phosphorus removal and impact of nitrite accumulation on phosphorus removal in a continuous anaerobic-anoxic-aerobic (A^{2O}) process treating domestic wastewater. Enzyme. Microb. Tech., 48 (2011) 134–142.
[29] R. Naseer, S. Abualhail, X. Lu, Biological nutrient removal with limited organic matter using a novel anaerobic-anoxic/oxic multi-phaed activated sludge process, Saudi J. Biol. Sci., 20 (2013) 11–21.
[30] Y. Chen, B. Li, L. Ye, Y. Peng, The combined effects of COD/N ratio and nitrate recycling ratio on nitrogen and phosphorus removal in anaerobic/anoxic/aerobic (A2/O)-biological aerated filter (BAF) systems, Biochem. Eng. J., 93 (2015) 235–242.
[31] W. Zhou, Y. Sun, B Wu, Y. Zhang, M. Huang, T. Miyanaga, Z. Zhang, Autotrophic denitrification for nitrate and nitrite removal using sulfur-limestone, J. Environ. Sci. 23 (2011) 1761–1769.
[32] X. Xu, C. Chen, A. Wang, W. Guo, X. Zhou, D.J. Lee, N. Ren, J.S. Chang, Simultaneous removal of sulfide, nitrate and acetate under denitrifying sulfide removal condition: modeling and experimental validation, J. Hazard. Mater., 264 (2014) 16–24.
[33] L. Ye, and T. Zhang, Bacterial communities in different sections of a municipal wastewater treatment plant revealed by 16S rDNA 454 pyrosequencing, Appl. Microbiol. Biotechnol., 97 (2013) 2681–2690.